Irrig Sci (1989) 10:63–71

Irrigation Science


# Determination of soil water content by X-ray computed tomography and magnetic resonance imaging*

S. H. Anderson and C. J. Gantzer

Department of Agronomy, University of Missouri, Columbia, MO 65211, USA

Received October 13, 1987

**Summary.** Experiments were conducted to compare the use of X-ray computed tomography (CT) and magnetic resonance imaging (MRI) methods for determining water content in soil. Soil cores of Mexico silt loam packed at bulk densities of 1.2, 1.3, 1.4, and 1.5 $Mg/m^3$ and Crider silty clay packed at bulk densities of 1.3, 1.4, 1.5, and 1.6 $Mg/m^3$ were evaluated using a CT scanner. Results indicate that the X-ray CT explained 98% of the variation in water content over a range from air-dry to saturation. Three attempts were made to obtain MRI scans of soil cores varying in soil water content. Two of these attempts were made with contrasting agents. No images were obtained of the soil cores during all three attempts. It is suggested that the failure to obtain images of soil cores is closely related to the settings of the pulse repetition time and the spin echo time on the MRI unit. The range in settings for these two parameters on the commercial MRI unit used in this study did not allow short increments to be selected and therefore it was not possible to obtain reconstructed images of the soil cores for this experiment. However accessibility to a prototype MRI unit should allow more conclusive work to determine the full capabilities of MRI for determining soil water content.

Measurement of soil water content on a macropore scale is required to obtain a detailed understanding of transport processes. Current methods for measuring soil water content limit the study of soil-plant root water transport since roots primarily function within a 1 to 2 mm thick rhizospere zone, through which all transport must occur. Therefore, a need exists for measurement techniques which allow rapid evaluation of water content of intact cores on a detailed level. Recent advances in X-ray computed tomography (CT) and nuclear magnetic resonance imaging (MRI) or nuclear magnetic resonance (NMR) imaging have allowed the development of methods for rapid nondestructive three-dimensional analysis of intact biological tissue (Hounsfield 1972; Bottomley et al. 1986). With X-ray CT, the intensity of a collimated X-ray

* Contribution from the Missouri Agricultural Experiment Station Journal No. 10424, Department of Agronomy, University of Missouri, Columbia, MO 65211, USA

beam passing through an object is measured by an array of detectors located opposite the X-ray source. MRI imaging methods use a strong static magnetic field and the decay of induced radio frequency (*rf*) radiation to measure changes in nuclear spin characteristics of biological and other materials which are related to the concentration and state of hydrogen protons (H-protons). If the principal source of H-protons is from water, then the H-proton concentration can be correlated with water content.

Computed tomography, whether from X-ray or MRI, is the method which uses a computer to reconstruct a tomographic plane (slice) of the specimen. The resolution of X-ray CT scanners is approximately 1 mm wide × 1 mm long × 3 mm thick, while the resolution of MRI scanners can be as detailed as 50 μm × 50 μm with a slice thickness of 1.25 mm (Johnson et al. 1986). Nondestructive monitoring of intact soil at similar resolutions provides a research method for evaluating interrelationships between soil structure and soil water content in three dimensions.

Applications of X-ray CT and MRI have not been limited to the field of medicine. Several investigators (Petrovic et al. 1982; Hainsworth and Aylmore 1983; Crestana et al. 1985; Hainsworth and Aylmore 1986; Anderson et al. 1988) illustrated the use of X-ray CT for the evaluation of soils. Hainsworth and Aylmore (1983) conducted preliminary studies to examine the possibility of using X-ray CT to measure spatial changes in soil water content related to soil-root water transport. They modified a gamma-ray unit and found results which compared favorably with those from an X-ray CT scanner. Hainsworth and Aylmore (1986) used the CT to show the effect of a single root on the removal of soil water. Crestana et al. (1985) showed that X-ray CT scanners could be used to measure the movement of water in soils at rates of 1.6 mm/s. Tollner et al. (1987) used an X-ray CT unit to observe soil pierced by a cone penetrometer. Anderson et al. (1988) studied methods of calibration for determining water content for two soils with differing iron contents.

Researchers have also illustrated the use of MRI for the nondestructive evaluation of water content in plants (Bottomley et al. 1986; Brown et al. 1986; Omasa et al. 1985). Bottomley et al. (1986) used a spatial resolution of 0.6 mm with an undefined slice definition to observe the movement of a dilute solution of $CuSO_4$ into and through roots of *Vicia faba*. Brown et al. (1986) were able to differentiate anatomical regions of the *Pelargonium hortorum* roots with a spatial resolution of 0.1 mm × 0.1 mm × 1.2 mm. Omasa et al. (1985) used MRI with a spatial resolution of 2 mm to image root seedlings and show changes in water content in the seedlings.

At present, little effort has been made to use MRI to measure water content in soil and to compare results with X-ray CT methods. Because of the greater spatial resolution of the MRI units, it would be useful to evaluate whether MRI can be used to determine water content in soil cores. The objectives of the study were to evaluate the use of MRI as a tool for measuring detailed water content in soil cores and to compare the results with X-ray CT for determining water content in soils.

## Materials and methods

Soil from the A horizon of Mexico silt loam (fine, montmorillonitic, mesic Udollic Ochraqualfs) and the B2t horizon of Crider silt loam (fine-silty, mixed, mesic Typic Paleudalfs) was obtained from continuous fallow plots (Jamison et al. 1968; Wendt et al. 1986) near Kingdom City, Missouri and from a field near Farmington, Missouri, respectively. Soil material was brought to

the lab, air-dried, and passed through a 2-mm sieve. Particle density was determined on 6 replicates for each soil using the method of Blake (1965). The particle size distribution for each soil was evaluated using the pipette method of Day (1965). The iron content of each soil was determined using energy dispersive spectroscopy (Smart and Tovey 1982).

The X-ray CT unit used for this investigation was a Philips Tomoscan 310. This scanner is a third generation (rotate/rotate) CT with 576 Xenon ionization detectors in the detector array. A 120 peak kilovoltage X-ray beam was utilized. Approximately 900 profiles were acquired in 4.8 s; and using a reconstruction field of view of 320 mm, each pixel in the resultant $256 \times 256$ pixel image corresponded to a volume element of $1.25 \times 1.25 \times 12$ mm. The reconstruction algorithm was filtered backprojection. Several researchers have presented the theory of X-ray CT (Brooks and Di Chiro 1975, 1976; Budinger and Gullberg 1974).

MRI scans were determined at 25.5 MHz on a commercial 0.6 Tesla (T) Technicare Teslacon MRI scanner. Images were reconstructed on a $192 \times 256$ array. The pulse repetition time ($T_R$) was 1,590 ms. The echo time ($T_E$) was 90 ms. Data acquisition time was 10 min. Two imaging pulse sequences were utilized, partial saturation and spin echo. Beall et al. (1984) and Johnson et al. (1986) present the details of the theory of MRI.

Experiments were conducted on both dry soil and wet soil using the X-ray CT scanner. Using air-dry soil, eleven cores, each 52 mm i.d. $\times$ 48 mm long, were packed at bulk densities of 1.2, 1.3, 1.4, and 1.5 Mg/m$^3$ with the Mexico soil and eleven soil cores each were packed at bulk densities of 1.3, 1.4, 1.5, and 1.6 Mg/m$^3$ with the Crider soil. Higher bulk densities were used for the Crider soil because of its greater particle density. The air-dried soil was pressed into 52 mm i.d. $\times$ 48 mm high PVC plastic cylinders. One of the eleven cores for each bulk density from each soil was dried in the oven at 105 °C and immediately stored in a dessicator until scanned. To fill the aperture-stage of the CT scanner with mass, a group of four cores were analyzed together. A water bag was wrapped around the group of cores to provide additional mass. Cores were arranged with two upper cores centered on top of two bottom cores separated by a 25 mm styrofoam board. Cores were arranged in a modified latin square design with relative position being the column and scan number the row. The mean attenuation coefficient and standard deviation were determined for a 13,950 mm$^3$ volume in the center of each core. Regression relationships between attenuation coefficients and volume fraction of solids for the oven-dry cores and the air-dry cores adjusted to an oven-dry basis were not significantly different. Therefore, the attenuation coefficients for the air-dry cores were adjusted to an oven-dry basis in subsequent analyses.

The wet soil experiment for the X-ray CT used exactly the same cores as the dry soil experiment. Distilled water was slowly added to 9 of the cores of each density group for both the Mexico and Crider soils. Water contents ranged from air-dry to saturated values. The water was added over an 8 h period, and subsequent to wetting, the bottom and top of the core were sealed with paraffin. Cores were then placed on their side in humid chambers and equilibrated for 2 weeks. Cores were rotated 180° every day for the 2 week period. After the water content in the soil cores had equilibrated, tomographs were taken using the same procedure as described for the dry soil experiment.

The image obtained using X-ray CT is a distribution of linear attenuation coefficients ($\mu$). When using CT for soil materials, the linear attenuation coefficient is related to the volume fractions of soil solids and water by the following expression:

$$\mu = f_s \mu_s + f_w \mu_w , \tag{1}$$

where $f_s$ *and* $f_w$ are the volume fractions of the soil solids and water, respectively, and $\mu_s$ and $\mu_w$ are the attenuation coefficients of the soil solids and water, respectively. In order to experimentally obtain the relationship between $\mu$ and $f_s$, the soil material must be oven-dry. Once the relationship between $\mu$ and $f_s$ has been determined, the attenuation due to $f_s$ may be subtracted to obtain a relationship between a new variable $\mu^*$ and $f_w$,

$$\mu^* = \mu - f_s \mu_s = f_w \mu_w , \tag{2}$$

where $\mu^*$ is the portion of the attenuation coefficient due to attenuation by water. (Note that $f_s$ is equivalent to the bulk density divided by the particle density and $f_w$ is the equal to $\theta$, the volume fraction of soil water.)

Three wet soil experiments were conducted using the MRI scanner. For the first experiment, 12 cores each were packed at a bulk density of 1.3 Mg/m$^3$ for the Mexico soil and at a bulk

density of 1.4 $Mg/m^3$ for the Crider soil. Distilled water was slowly added to 10 of the soil cores from each soil as in the X-ray CT experiment to obtain water contents from air-dry to satiation. These cores were sealed with paraffin and equilibrated as before and MRI scans were taken. Because poor results were obtained, two subsequent experiments were conducted substituting contrasting agents for distilled water. Two groups of cores were packed as before for each of the soils. Instead of adding distilled water, 20% (by wt.) $CuSO_4$ solution was added to one group of cores (10 for each soil) and 0.01% (by wt.) $Cu(NO_3)_2$ solution was added to the other group of cores. (The soil cores were oven-dried prior to adding the solutions to assure equal concentrations of solution throughout the cores.) The soil cores were then sealed with paraffin and equilibrated and MRI scans were taken.

Swelling was noted for both the Mexico and Crider soils upon addition of water. Therefore, swelling behavior was evaluated on separate cores using a point gauge to measure changes in vertical swelling of laterally confined samples. Regression relationships were developed and used to determine correct bulk densities and volumetric soil water contents for soil cores in the wet soil experiments.

## Results and discussion

Measured data for selected physical and chemical properties for the soil material from the A horizon of the Mexico silt loam and the B2t horizon of the Crider silt loam are given in Table 1. The principal differences between the two soil materials are the higher amount of clay content and iron oxides in the Crider soil. The greater iron oxide content in the Crider is the probable cause for the higher particle density of the Crider soil.

### *X-ray CT experiment*

The relationships between the attenuation coefficients and $f_w$ as influenced by bulk density for the Mexico and Crider soils are illustrated in Figs. 1 and 2, respectively. The reason for the nonparallel lines for both soils is swelling since these values have not been corrected for swelling effects. However, even uncorrected for swelling, the correlation coefficients are all greater than 0.93. Some nonlinear behavior appears to be present for each of the bulk density relationships in Figs. 1 and 2.

Because swelling problems occurred for these soils when water was added, the water contents and bulk densities were corrected using regression relationships deter-

**Table 1.** Selected physical and chemical properties for the Mexico silt loam A horizon and Crider silt loam B2t horizon

| | | | Textural particle | | | | | |
|---|---|---|---|---|---|---|---|---|
| Soil | Horizon | Depth (m) | Class | Density ($Mg/m^3$) | Sand (kg/kg) | Silt (kg/kg) | Clay (kg/kg) | $Fe_2O_3$-content* (kg/kg) |
| Mexico | A | 0–0.15 | silt loam | 2.63 | 0.033 | 0.743 | 0.224 | 0.0143 |
| Crider | B2t | 0.45–1.00 | silty clay | 2.75 | 0.043 | 0.474 | 0.483 | 0.0536 |

* $Fe_2O_3$ content was calculated from total Fe determined by energy dispersive spectroscopy with an electron microscope

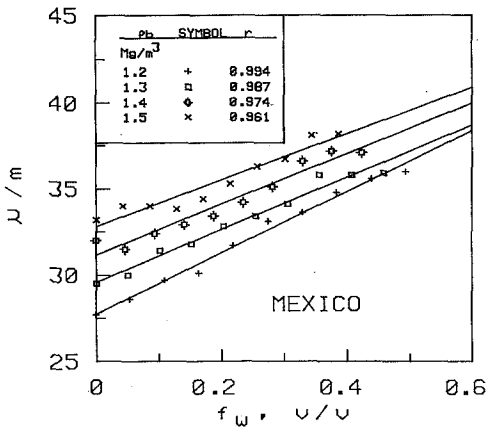


**Fig. 1.** Relationships between $\mu$ (attenuation coefficient) and $f_w$ (volume fraction of soil water) for selected bulk densities of Mexico soil. The $f_w$ are not corrected for swelling

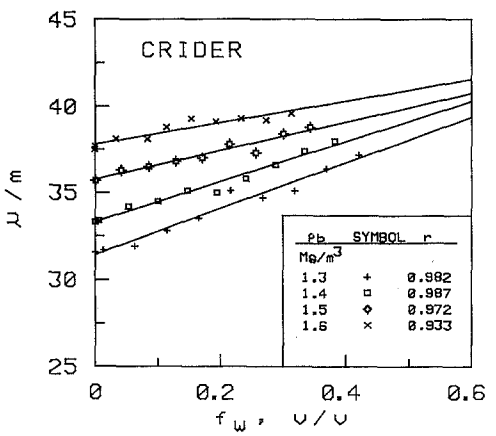


**Fig. 2.** Relationships between $\mu$ (attenuation coefficient) and $f_w$ (volume fraction of soil water) for selected bulk densities of Crider soil. The $f_w$ are not corrected for swelling

mined experimentally. The coefficients of determination were all greater than 0.95 for these equations. Attenuation coefficients were corrected for $f_s$ using the relationships obtained from the dry soil experiment. This procedure was equivalent to using Eq. (2). The relationships between attenuation coefficients corrected for the volume fraction of soil solids and volume fraction of soil water for the Mexico and Crider soils are shown in Figs. 3 and 4, respectively. About 98% of the variation in attenuation coefficients due to water content was explained by $f_w$. It is interesting to note that the slopes of the lines for each soil are nearly identical (17.7 $m^{-1}$ for Mexico and 17.9 $m^{-1}$ for Crider). However, the values are less than 19 $m^{-1}$, the value which is often used as the standard attenuation coefficient of water. It is also noted that the intercept for the Mexico soil ($-0.2$ $m^{-1}$) is not significantly different from zero; while the intercept for the Crider soil (0.6 $m^{-1}$) is significantly different from zero. This suggests that although the portion of the attenuation due to the soil solids was subtracted from both soils, the attenuation due to water is slightly different between the soils.

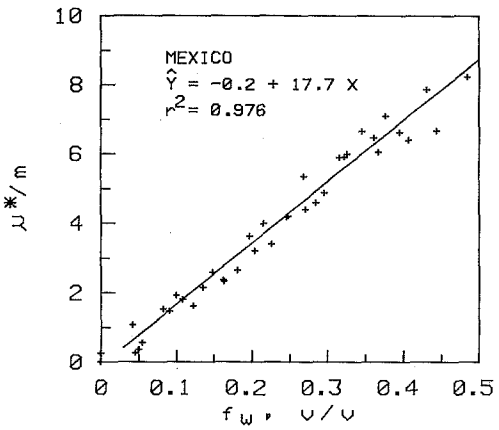


**Fig. 3.** Relationship between $\mu^*$ (adjusted attenuation coefficient) and $f_w$ (volume fraction of soil water) for the Mexico soil. The attenuation coefficients are adjusted for $f_s$ and the $f_w$ are corrected for swelling

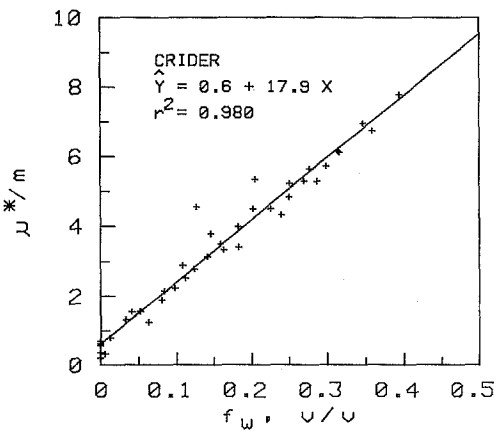


**Fig. 4.** Relationship between $\mu^*$ (adjusted attenuation coefficient) and $f_w$ (volume fraction of soil water) for the Crider soil. The attenuation coefficients are adjusted for $f_s$ and the $f_w$ are corrected for swelling

*MRI experiment*

Three attempts were made to obtain MRI scans of the soil cores varying in soil water content. In the first, soil cores which had distilled water added were imaged along with a MRI standard [0.01% (by wt.) $Cu(NO_3)_2$ solution]. Although the image indicated the position of the standard, no images of the soil cores could be obtained. We felt this was due, in part, because we had not used a constrasting agent as had been used in the known standard. Two other attempts were made to obtain NMR images using 20% (by wt.) $CuSO_4$ solution and 0.01% (by wt.) $Cu(NO_3)_2$ solution for saturating the soil. No images were obtained for the soil cores in either case. For the cores with 20% $CuSO_4$, extreme distortions of the images of the standards occurred due to the high concentration of metal.

It is suspected that failure to obtain images of soil cores is closely related to the setting of the pulse repetition time ($T_R$) and the echo time ($T_E$) which were too long to obtain reconstruction images of the soil cores, even with contrasting agents. Paetzold et al. (1985) suggested values of $T_1$ and $T_2$ for water content in soils which are much smaller than those typical for biological materials. Since the MRI unit used for

**Table 2.** Comparison of X-ray CT and MRI methods for measurement of soil water content

| X-ray CT | | MRI | |
|---|---|---|---|
| Advantages | Disadvantages | Advantages | Disadvantages |
| Theoretically simpler | Uses ionizing radiation | Uses nonionizing radiation | Theoretically complex |
| Measures bulk density | Beam hardening | Differentiates between materials | Relatively inaccessible |
| Applicable for high iron content soils | Doesn't differentiate between materials | Discriminates between states of water | Cannot use with metal |
| Fast (2 to 4 s) | | Discriminates between | Practical interpretation |
| Provides digital output | | biological material and soil | is still in its infancy |
| More accessible | | Finer resolution | Exclusively qualitative |

the experiment is dedicated to medical use, significant reductions of the $T_R$ and $T_E$ to an appropriate range for soils was not possible. Tollner and Rollwitz (1988) found similar results to those from this study using MRI to evaluate soil water in two coarse-textured soils. Rogers and Bottomley (1987) found that soil water was essentially invisible in seven natural soils with MRI even when using a broad range of soil water contents to near saturation. Although these results are discouraging for the potential application of MRI for measurement of soil water content, the results are encouraging for evaluation of roots systems with MRI since root water is visible and soil water is invisible with MRI which provides excellent root-to-soil image contrast (Rogers and Bottomley 1987). Material imaging instruments/accessories may be developed in the future by MRI instrument manufacturers which should be more suitable for measuring soil water content.

## Conclusions

Results show that X-ray CT can be used to determine water content of intact soil. Approximately 98% of the variation in CT attenuation by the soil cores for each of the two soils were accounted for by regression relationships with $f_w$ after correcting for swelling effects and $f_s$. MRI did not produce usable results probably due to equipment constraints in setting pulse repetition and echo times to the appropriate range for soil water. Table 2 illustrates a qualitative comparison between the X-ray CT and MRI methods for determining water content in soils. Although MRI methods have some limitations, there are some advantages over the X-ray CT methods, especially in discriminating between the energy status of soil water. Further research needs to be conducted to evaluate the full potential of MRI for soil water content analysis. From this experiment, it appears that the use of X-ray CT is a better tool to monitor water content in soils. However, if accessibility to a prototype NMR unit were possible, more conclusive work could be conducted to determine the full capabilities of MRI for determining soil water content.

Although these results demonstrate the potential of X-ray CT for laboratory studies involving soil-water systems, work is underway to develop portable CT units for field use. Thus Miller (1988) has developed a portable computed tomography unit at the University of Missouri for field use which has been used for evaluating structural defects on wooden utility poles.

## References

Anderson SH, Gantzer CJ, Boone JM, Tully RJ (1988) Rapid nondestructive bulk density and soil water content determination by computed tomography. Soil Sci Soc Am J 52:35

Beall PT, Amtey SR, Kasturi SR (1984) NMR data handbook for biomedical applications, chapter 2. Basic physics for NMR and NMR imaging. Pergamon Press, New York, p 11

Blake GR (1965) Particle density. Methods of soil analysis, part 1. Agronomy 9:371

Bottomley PA, Rogers HH, Foster TH (1986) NMR imaging shows water distribution and transport in plant root systems in situ. Proc Natl Acad Sci USA 83:87

Brooks RA, Di Chiro G (1975) Theory of image reconstruction in computed tomography. Radiology 117:561

Brooks RA, Di Chiro G (1976) Principles of computer assisted tomography (CAT) in radiographic and radioisotopic imaging. Phys Med Biol 21:689

Brown JM, Johnson GA, Kramer PJ (1986) In vivo magnetic resonance microscopy of changing water content in *Pelargonium hortorum* roots. Plant Physiol 82:1158

Budinger TF, Gullberg GT (1974) Three dimensional reconstruction in nuclear medicine emission imaging. IEEE Trans Nucl Sci 21:2

Crestana S, Mascarenhas S, Pozzi-Mucelli RS (1985) Static and dynamic three-dimensional studies of water in soil using computed tomographic scanning. Soil Sci 140:326

Day PR (1965) Particle fractionation and particle size analysis. Methods of soil analysis, part 1. Agronomy 9:545

Hainsworth JM, Aylmore LAG (1983) The use of computer-assisted tomography to determine spatial distribution of soil water content. Aust J Soil Res 21:435

Hainsworth JM, Aylmore LAG (1986) Water extraction by single plant roots. Soil Sci Soc Am J 50:841

Hounsfield GN (1972) A method of and apparatus for examination of a body by radiation such as X- or gamma-radiation. Brit Pat No 1283915, London

Jamison VC, Smith DD, Thornton JF (1968) Soil and water research on a claypan soil. USDA-ARS Tech Bull 1379, U.S. Government Printing Office, Washington, DC

Johnson GA, Thompson MB, Gewalt SL, Hayes CE (1986) Nuclear magnetic resonance imaging at microscopic resolution. J Magnet Reson 68:129

Miller WH (1988) Design and implementation of a portable computerized axial tomography system for field use. Nucl Instrum Methods (In press)

Omasa K, Onone M, Yamada H (1985) NMR imaging for measuring root systems and soil water content. Environ Control Biol 23:99

Paetzold RF, Matzkanin GA, De Los Santos A (1985) Surface soil water content measurement using pulsed nuclear magnetic resonance techniques. Soil Sci Soc Am J 49:537

Petrovic AM, Siebert JE, Rieke PE (1982) Soil bulk density analysis in three dimensions by computed tomographic scanning. Soil Sci Soc Am J 46:445

Rogers HH, Bottomley PA (1987) In situ nuclear magnetic resonance imaging of roots: Influence of soil type, ferromagnetic particle content, and soil water. Agron J 79:957

Smart P, Tovey NK (1982) Electron microscopy of soils and sediments: techniques. Oxford University Press, New York, pp 161–163

Tollner EW, Rollwitz WL (1988) Pulse NMR for quantifying moisture in agricultural materials. Trans Am Soc Agric Eng (In press)

Tollner EW, Verma BP, Cheshire JM (1987) Observing soil tool interactions and soil organisms using X-ray computer tomography. Trans Am Soc Agric Eng 30:1605

Wendt RC, Alberts EE, Hjelmfelt AT (1986) Variability of runoff and soil loss from fallow experiment plots. Soil Sci Soc Am J 50:730